Rupture propagation, dynamical front selection, and the role of small length scales in a model of an earthquake fault

Christopher R. Myers and J. S. Langer
Institute for Theoretical Physics, University of California, Santa Barbara, California 93106-4030
(Received 19 November 1992)

We examine a model of rupture propagation on a one-dimensional earthquake fault, focusing both on the role of small length scales in controlling the dynamics and on the mechanisms by which propagating modes are selected. In order to obtain a well-defined continuum theory, we add a small amount of viscous dissipation to a previously studied model in which rupture propagation was controlled by a finite-difference grid spacing. We find that the dynamically selected rupture mode is one in which nearly free slip occurs in a pulse whose speed and shape are determined by a novel selection mechanism.

PACS number(s): 91.30.Mv, 03.40.−t, 46.30.Nz, 62.20.Mk

I. INTRODUCTION

The uniform Burridge-Knopoff (BK) model [1] of an earthquake fault has recently been shown to exhibit a rich diversity of dynamic behavior [2–4]. In particular, Langer and Tang (LT) [4] have demonstrated that the long-range propagation of sharp rupture fronts typically associated with large-magnitude events in these models resembles front propagation into unstable or metastable states in other dynamical systems [5–11]. LT found two particularly interesting features of propagating ruptures in these earthquake models: the existence of a linear marginal-stability mechanism governing the dynamical selection of ruptures which propagate into unstable states, and the dependence of the selected speeds and spatial profiles of the rupture fronts on a short-wavelength cutoff, without which the dynamics of the system are undetermined [4]. In this paper, we introduce a related model with a different small length-scale cutoff, and study in greater detail the dynamics of rupture propagation in that model. We find that a novel selection mechanism governs the dynamical selection of propagating fronts.

The need for a small length-scale cutoff arises from an instability to the formation of infinitely sharp shock fronts in fault models with velocity-weakening friction. In their earlier work, LT chose as the small-scale cutoff a finite-difference grid spacing used in the numerical integration of the underlying model partial differential equation. This length scale arises plausibly from the original conception of the BK model as a "block and spring" model. With such a choice, the selected rupture speed depends on the grid spacing a in such a way that the velocity v approaches the sound speed $c \equiv 1$ from above as $a \to 0$. Within the framework of continuum elasticity theory, however, one must address the problem of how to regularize singularities which develop at small length scales. Finite-difference grid spacings are one such choice, but we will examine another here.

In this paper, we introduce a short-wavelength cutoff which is more natural than the finite-difference grid spacing considered previously. In particular, we add a simple viscous dissipation to the one-dimensional uniform BK model and investigate the dynamics of propagating ruptures. This added term smooths the dynamics on some viscous length scale, and, with the introduction of such a scale, the rupture dynamics becomes independent of the grid spacing a (which always exists in finite-difference integrations) as long as the smoothing scale is sufficiently larger than the grid spacing. The resulting model has a well-defined continuum limit as $a \to 0$, and the rupture dynamics is instead determined by the viscous length scale. In the manner undertaken previously [4], we perform a marginal-stability analysis to determine the propagation speed of ruptures at threshold. Unlike in the previous work, however, we solve a continuum model of the dynamics and demonstrate that simulated ruptures (with both the added viscosity and an underlying finite-difference grid) move in a manner predicted by the continuum model and independently of the grid spacing a.

In addition to examining the linear marginal-stability mechanism at threshold (i.e., for the propagation of a rupture into an unstable state), we investigate the nature of steady-state solutions for propagation off threshold, into a metastable state. Whereas there often exists only a discrete set of steady-state fronts for propagation into a metastable state (in other systems) [9], we find that the multivalued static friction which causes ruptures to restick allows a continuum of steady-state propagating solutions off threshold with different velocities, one of which is selected dynamically.

The larger questions which provide the backdrop for this paper are these: Under what conditions do steady-state propagating solutions in various models exist, and how many solutions are there? What is the spatial character of such solutions, and what is their stability? (Of interest to the seismological community, for example, is whether earthquake slip occurs in a localized "self-healing" pulse which propagates along the fault [12], or in a extended manner such that a large region of the fault ruptures and remains unstuck for a time comparable to that of the entire event.) Under what conditions is a particular solution selected dynamically (from, say, a continuum of possible solutions)? How does the character of propagating ruptures differ among related models? (In

models of propagating cracks without an unstable velocity-weakening friction [13], for example, the selection of modes is quite different.) In this paper, we address some of these questions within the context of our viscous one-dimensional model of earthquake faults.

In Sec. II, we briefly review previous work on the one-dimensional BK model studied in Refs. [2] and [3], focusing on the manner in which the finite-difference grid spacing a controls the rupture dynamics. Section III contains an extended analysis of the new model with viscosity. Here, we examine both the linear marginal stability of threshold propagation and the character of selected modes off threshold, and we discuss some physical features of the propagating front that emerges from our theory. In Sec. IV, we digress somewhat to address the assumptions we have made regarding viscoelastic response, and in Sec. V we compare the effects of the finite-difference and viscous length scales. In Sec. VI we summarize the paper and describe some open questions.

II. RUPTURE PROPAGATION IN THE UNIFORM BURRIDGE-KNOPOFF MODEL

We briefly review the results of LT [4] investigating the nature of rupture propagation in the uniform BK model. These results provide a useful introduction to the new investigation described in Sec. III.

We consider initially a partial differential equation describing the dynamics of a scalar displacement field $u(x,t)$:

$$\ddot{u}=u''-(u-\Delta)-\phi(\dot{u}) , \tag{1}$$

where

$$\phi(\dot{u})=\begin{cases}(-\infty,\phi_{\max}\equiv 1], & \dot{u}=0\\ 1-2\alpha\dot{u}, & 0<\dot{u}\le 1/(2\alpha)\\ 0, & \dot{u}>1/(2\alpha) .\end{cases} \tag{2}$$

This is the uniform (spatially homogeneous) BK model studied in Ref. [4], with the single change in notation being that we have introduced an explicit loading parameter Δ so that $u=0$ along the unruptured part of the fault. Note that, when the friction ϕ is absent, (1) is a massive wave equation in which the mass—the inverse of some characteristic length such as the crust depth in the earthquake problem—has been scaled to unity, as has the wave speed. (All rupture velocities are measured in units of that scaled wave speed.) To simulate a fault loaded through the motion of tectonic plates, one could make Δ a function of time as was done in Ref. [2]. The piecewise linear friction $\phi(\dot{u})$ is the same as in Ref. [4], but differs from the other, more smoothly varying nonlinear forms investigated in Refs. [2] and [3]. The important elements of the friction are preserved, however, namely the multivalued sticking force at $\dot{u}=0$ and the velocity-weakening character (for $\alpha>0$) during slip. The multivalued static friction allows resticking behind the open rupture, and the velocity-weakening sliding introduces an essential instability.

We consider situations in which a rupture propagates through a region where, initially, $u=0$. Then, if $\Delta=\phi_{\max}=1$, the region ahead of the rupture front is unstable in that $\phi[\dot{u}(x)]=1$ for x ahead of the tip. We define ϵ as

$$\epsilon\equiv 1-\Delta , \tag{3}$$

so that the threshold case $\Delta=1$ corresponds to $\epsilon=0$. For smaller loadings, $\epsilon>0$, the region ahead of the tip is stable and requires contact with the front to reach the static friction limit $\phi_{\max}$ [14].

In a finite-difference approximation that is appropriate for numerical studies, Eq. (1) becomes

$$\ddot{u}_j=\begin{cases}0, & \dot{u}_j=0\\ \frac{1}{a^2}(u_{j+1}-2u_j+u_{j-1})-u_j+2\alpha\dot{u}_j-\epsilon, & 0<\dot{u}_j\le 1/(2\alpha)\\ \frac{1}{a^2}(u_{j+1}-2u_j+u_{j-1})-u_j+1-\epsilon, & \dot{u}_j>1/(2\alpha) ,\end{cases} \tag{4}$$

where a is the grid spacing. Let us restrict our attention to the region at the front of the rupture where slipping is taking place but where the speeds are small enough that $0<\dot{u}_j\le 1/(2\alpha)$, i.e., the second case in Eq. (4). In this effectively linear regime, solutions of (4) have the form

$$u_j(t)=A(q)\exp(qaj+\Omega t) , \tag{5}$$

where Ω is a solution of

$$\Omega^2-2\alpha\Omega+1-\frac{2}{a^2}[\cosh(qa)-1]\approx\Omega^2-2\alpha\Omega+1-q^2-\frac{a^2}{12}q^4+\cdots=0 . \tag{6}$$

The second, approximate form for (6) is useful for seeing how the small length scale a enters as the coefficient of a higher-order term in this dispersion relation.

LT [4] hypothesized that, in the threshold case $\epsilon=0$, there exists a continuum of steady-state propagating solutions characterized by different velocities v, and that a particular propagating mode is selected dynamically by the linear marginal-stability mechanism. They demonstrated that the predictions of this hypothesis were consistent with the results of numerical simulations of (4). This analysis supposes that an exponential rupture front of the form (5) moves along the x axis at speed $-v^*$, and that both v^* and the associated real spatial growth rate

q^* are determined by the relations

$$\Omega(q^*)=v^*q^*, \quad \left.\frac{\partial\Omega}{\partial q}\right|_{q=q^*}=v^* . \tag{7}$$

Equivalently, we can look for a double root of the equation

$$b^2q^2-2\alpha vq+1-\frac{a^2}{12}q^4+\cdots=0, \quad b^2\equiv v^2-1 , \tag{8}$$

with both $q=q^*$ and $v=v^*$ positive. Inspection of (8) shows that such a double root exists only for $v^*>1$ and $a\neq 0$. In the limit of small a,

$$q^*\approx\left[\frac{12\alpha}{a^2}\right]^{1/3}, \quad (v^*)^2\approx 1+(\tfrac{3}{2}\alpha a)^{2/3} , \tag{9}$$

so that the front becomes infinitely sharp ($q^*\to\infty$) and the propagation speed approaches the sound speed ($v^*\to 1$) as $a\to 0$.

The analysis of LT for the more general situation with $\epsilon>0$ was more speculative. The difficulty is that, when the unruptured part of the fault is not everywhere at the slipping threshold, an exponential front of the form Eq. (5) cannot extend indefinitely far into the region ahead of the rupture but must terminate at some point, also moving at speed $-v$, where the transition from sticking to slipping is taking place [15]. This is not easy to describe in a finite-difference where the elements ("blocks") are discrete and the slipping events occur at some (large) frequency v/a. It is at this point that the advantage of using a well-defined continuum model becomes particularly clear. Our investigation of off-threshold mode selection in the continuum model, to be described in Sec. III B, has revealed a great deal more about this mechanism than was apparent in LT. In short, LT seem to have made a lucky guess. Accordingly, it is best to postpone further discussion of this mechanism until later in the paper.

III. ONE-DIMENSIONAL MODEL WITH VISCOSITY

To the continuum equation (1) we add a viscous dissipation of the form $\eta\dot{u}''$:

$$\ddot{u}=u''-u+\Delta-\phi(\dot{u})+\eta\dot{u}'' , \tag{10}$$

where $\phi(\dot{u})$ is specified in Eq. (2). The added term $\eta\dot{u}''$ is a one-dimensional Kelvin viscosity that acts to smooth spatial variations in the velocity field $\dot{u}$.

This viscosity has been introduced to provide both a mechanism for dissipation and a small smoothing length scale. We do not claim that this term represents a completely realistic description of the viscoelastic response of a rupturing or fracturing brittle material; rather we intend it as a simple example of such a response which has the important feature of introducing a small controlling length scale. Numerical analysts often add an artificial viscosity of this form to simulations of systems exhibiting shocks in order to control those shocks, but we do not include this term only to alleviate computational burdens. More generally, we recognize that some form of dissipation is likely to smooth the dynamics and that rupture propagation in these models depends crucially on such smoothing.

A. Linear marginal stability at threshold

To solve for the dynamics of rupture propagation at threshold $\epsilon=0$, we proceed as in Ref. [4] with a linear marginal-stability analysis. In particular, after writing $u(x,t)=A(q)\exp(qx+\Omega t)$, we seek a wave number $q=q^*$ and velocity $v=v^*$ which satisfy Eqs. (7), where Ω is the solution of

$$\Omega^2-(\eta q^2+2\alpha)\Omega+1-q^2=0 . \tag{11}$$

In this case, the problem reduces to setting $\Omega=vq$ and then finding a double root of the equation

$$b^2q^2-2\alpha vq+1-\eta vq^3=0 \tag{12}$$

with positive $q=q^*$ and $v=v^*$. Note that the viscosity η, just like the correction of order a^2 in (8), introduces the higher-order term which permits solutions for finite q^*. Again these solutions exist only for $v^*>1$ and $\eta>0$. For η very small, the analogs of (9) are

$$q^*\approx\left[\frac{2\alpha}{\eta}\right]^{1/2}, \quad (v^*)^2\approx 1+(8\alpha\eta)^{1/2} . \tag{13}$$

We have solved Eqs. (7) numerically, using the dispersion relation (11), and have plotted the marginally stable velocity v^* as a function of the viscosity η in Fig. 1, for two values of the friction parameter α. We have also shown in Fig. 1 the results of numerical simulations of Eq. (10) to demonstrate that the velocities selected by direct numerical integration of the equation of motion agree with those predicted by the linear marginal-stability analysis. We have also verified that simulated

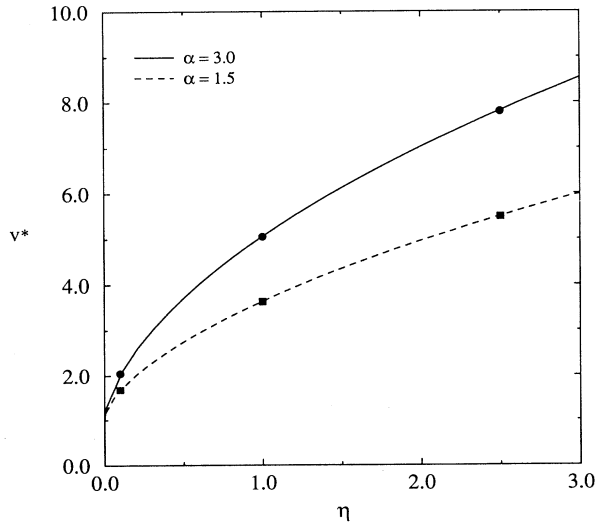

FIG. 1. Rupture velocity v^* predicted from linear marginal stability [Eq. (7)] at threshold ($\Delta=1$) and the asymptotic steady-state rupture velocities as measured in simulations of Eq. (14). The lines represent predicted velocities as functions of η for $\alpha=1.5$ and 3.0, as indicated, while the symbols indicate the results of simulation.

rupture fronts decay with the same rate q^* as that predicted by linear marginal stability.

There are three roots to the cubic equation (12) and, in the frame moving at velocity $-v$, the displacement u must have the form $u(x)=\sum_{i=1}^{3} A_i \exp(q_i x)$ in the region of interest. For $v=v^*$ and small η, $q_1 \approx 1/(2\alpha)$ and $q_2=q_3=q^* \approx b^2/(2\eta v)$. For small η, therefore $q^* \gg q_1$, and we would nominally expect that the slowly decaying mode $\exp(q_1 x)$ would dominate asymptotically as $x \to -\infty$. Linear marginal stability, however, predicts that the front decays exponentially as $\exp(q^* x)$. The selection of the marginally stable mode with $q=q^*$ and $v=v^*$ must therefore also ensure that the amplitude of the slowly decaying root A_1, be zero.

The numerical simulations whose results we show in Fig. 1 require a finite-difference approximation to the continuum equation (10); that is, we perform an integration of the finite-difference equations

$$\ddot{u}_j=\frac{1}{a^2}(u_{j+1}-2u_j+u_{j-1})-u_j+\Delta - \phi(\dot{u}_j)+\frac{\eta}{a^2}(\dot{u}_{j+1}-2\dot{u}_j+\dot{u}_{j-1}) . \quad (14)$$

But whereas in the original model (4) the rupture velocity always depends on the size of the finite-difference spacing a, our simulations reveal that the selected velocities and wave numbers are independent of a for sufficiently small a. In Sec. V we return to a discussion of the rupture dynamics in simulations where a is large compared to the viscous length $(q^*)^{-1} \approx [\eta/(2\alpha)]^{1/2}$.

B. Off-threshold selection in the viscous model

The linear marginal-stability analysis presented above describes the motion of the rupture front at threshold $\epsilon=0$. In a variety of systems [7,9], the dynamics of a front propagating into an unstable state are typically governed by linear marginal stability because the tip extends infinitely far ahead of the front and the behavior of the entire system is determined by the dynamics of the leading edge. In this case, there exists a continuum of stable steady-state propagating solutions of different velocities, the slowest of which is selected dynamically. For a front propagating into a metastable state, however, the nonlinearity behind the tip becomes relevant, and there is typically only a single steady-state propagating solution (or a discrete set of such solutions) [8–10]. We find, however, that in this class of earthquake models there exists a continuum of steady-state solutions off threshold, for $\epsilon>0$. We have not fully investigated the stability of these solutions, but it is clear that the state which is selected dynamically is the fastest of these solutions.

We are interested in steady-state solutions to Eq. (10), that is, solutions of the form $u(x+vt)$ moving at constant velocity $-v$. Such states are solutions of the third-order ordinary differential equation (ODE)

$$\eta v u'''-b^2 u''-u-\phi(vu')=-1+\epsilon , \quad (15)$$

subject to the boundary conditions $u(0)=u'(0)=u''(0)=0$, $x=0$ now being the instantaneous location of the rupture tip. For fixed η and α, we can look for solutions to (15) at different velocities v. Shown in Fig. 2 are the steady-state slipping rates $\dot{u}(x)=vu'(x)$ for various v, integrated forward in x starting at $x=0$. We find that there is a critical velocity v_c above which solutions cease to exist, or at least become highly extended, irregular, and nonphysical. For the particular parameter values chosen ($\alpha=3.0$, $\eta=0.1$, and $\epsilon=0.01$), we find $v_c=1.843\,71\pm0.000\,01$. For $v \le v_c$, there are steady-state solutions which restick; for these solutions, $vu'(x)=0$ for all x beyond the resticking point x_r and $u(x)$ is accordingly constant for $x>x_r$. For those resticking solutions with $v<v_c$, the existence of a singular third derivative $u'''(x)$ at the resticking point requires that the friction likewise be singular: $\phi \sim -|u''(x_r)|\delta(x-x_r)$. This singularity is permitted because arbitrarily large negative values of ϕ are allowed mathematically within our model.

We have included in Fig. 2 the slip pulse $\dot{u}(x)$ to which a full integration of the partial differential equation (PDE) (10), or more precisely, the finite-difference equation (14), converges at long times. The selected solution appears to be that which just barely resticks. At $v=v_c, u''(x_r)=0$, resticking is smooth and requires no divergence in ϕ. This "edge solution" which barely resticks is the fastest steady-state solution available to the system at fixed η and α. Because of resticking and the singular friction force in our model, there exists a continuous set of solutions off threshold rather than only the single solution which might be expected otherwise.

We have examined numerically the selection of off-threshold solutions by using the steady-state solutions for $u(x)$, $\dot{u}(x)$, and $\ddot{u}(x)$ generated by Eq. (15) as initial conditions for a full dynamic integration of Eq. (14). We

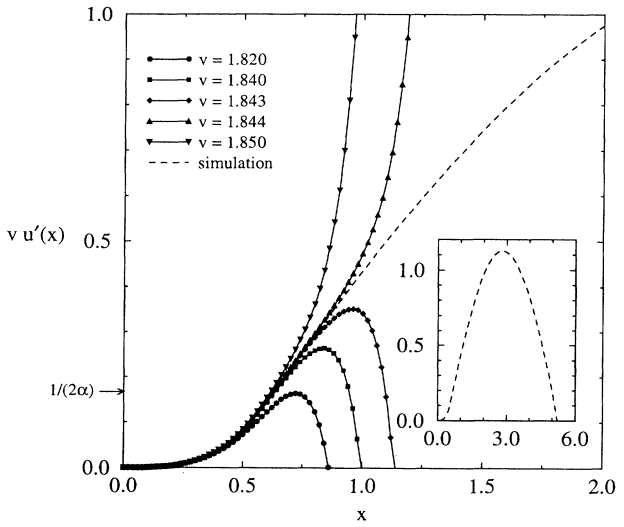

FIG. 2. Slip rates $\dot{u}(x)=vu'(x)$ for steady-state propagating solutions, as generated by a numerical integration of the third-order ODE (15), for various velocities v (solid curves with symbols). Also shown (dashed curve) is the asymptotic steady state $\dot{u}(x)$ exhibited in the dynamical simulation of the PDE (10). The results shown are for $\alpha=3.0$, $\eta=0.1$, and $\epsilon=0.01$. The inset shows the full width of the dynamically selected pulse, which is considerably larger than the pulse widths shown for $v<v_c$.

present the results of these simulations in Fig. 3, which shows the time evolution of slip pulses $\dot{u}(x)$ for two different initial conditions. The steady-state edge solution with $v=v_c$ is preserved under the equation of motion, while the "subedge" solution with $v<v_c$ is attracted at long times to the edge solution.

The apparent instability of the singular steady-state solutions with $v<v_c$ in the fully dynamic integration of Eq. (14) raises several unresolved questions. While those singular solutions are mathematically allowed within our model, and can be studied within the context of the ODE (15), it is not obvious that such solutions will be accessible in any finite-difference approximation, or in any finite time-step integration that discretizes the times at which individual points on the fault can restick. Any finite-difference scheme (with or without the smoothing viscosity that we have introduced) may smooth a singular solution. The instability of subedge solutions demonstrated in Fig. 3 may therefore suggest that once the singular resticking point is smoothed, the only remaining smooth solution to be found is the edge solution at $v=v_c$.

It is possible, of course, that the slower steady-state solutions are simply unstable, but we have not as yet been able to answer this question. If the slower steady-state solutions with discontinuous second derivative are being treated appropriately in the finite-difference model (14), then we would wish to determine if the edge solution is selected from among a set of stable states (by a mechanism such as marginal stability) or if it is simply an isolated stable attractor for the dynamics.

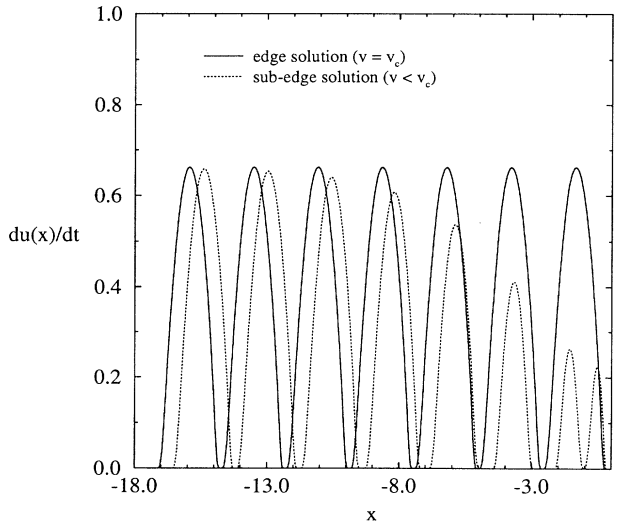

FIG. 3. Time evolution of slip pulses $\dot{u}(x,t)$ moving to the left for two initial conditions: the edge solution at $v=v_c$ (solid curves) and a steady-state solution of Eq. (15) for $v<v_c$ (dotted curves). Shown are snapshots of each pulse taken at fixed time intervals of $\Delta t=2.0$. For both cases, $\alpha=3.0$, $\eta=0.1$, and $\epsilon=0.5$. The edge solution moves at constant velocity $v_c\approx 1.215$ while the subedge solution both changes shape over time and accelerates to reach the edge solution. The initial condition for the subedge case was the solution of the ODE (15) for $v=1.10$. The bunching of pulses in the subedge case at short times reflects its initially slow velocity.

Regardless of such issues, we can postulate that the edge solution is the one which is selected dynamically, such that $v=v_c$. This hypothesis appears to be correct within the accuracy of our numerical experiments. In Fig. 4, we plot $v(\epsilon)$, the velocity of the edge solution to Eq. (15) for various ϵ, along with values of v obtained by full integration of the finite-difference approximation (14) to the PDE (10). We find agreement with the simulation at all ϵ, with no free parameters to fit.

In Ref. [4], LT hypothesized that the selection of modes off threshold was determined by the only characteristic slip-rate scale in the friction $\phi(\dot{u})$. In particular, they supposed that the selected steady-state solution was that for which the maximum slip rate $\dot{u}_{\max}\approx 1/(2\alpha)$. The rupture speeds $v(\epsilon)$ predicted with this hypothesis agreed unexpectedly well with those found in simulations, with the minor caveat that the free parameter denoted by γ in Ref. [4] was adjusted to fit the data and was found to be slightly different than its analytically predicted value. With this hypothesis, LT also were able to demonstrate how this selection mechanism at $\epsilon>0$ merges smoothly with the linear marginal stability mechanism at $\epsilon=0$.

Figure 2 demonstrates that slip rates $\dot{u}$ exceed $1/(2\alpha)$ considerably for solutions with $v\approx v_c$. Why, then, did the LT hypothesis work as well as it did? The answer lies in the great sensitivity of the steady-state solutions to small variations of v in the vicinity of v_c. For the small values of η that we have studied, small differences in v separate the solution with $\dot{u}_{\max}=1/(2\alpha)$ and the edge solution at $v=v_c$. This sensitivity arises from the character of the solutions of Eq. (15).

For $0<\dot{u}<1/(2\alpha)$, $u(x)$ is a linear superposition of three exponential modes of the form $\exp(qx)$, where the

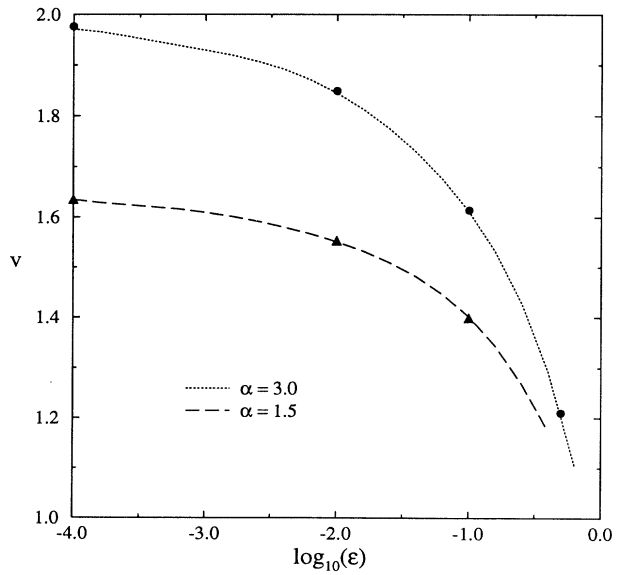

FIG. 4. Rupture velocity v as a function of the loading parameter ϵ, for $\eta=0.1$ and various α, as indicated. The curves represent the velocities of the edge solutions of the ODE (15). The symbols represent asymptotic steady-state velocities measured in a dynamical simulation of the PDE (10).

q's are the three roots of Eq. (12). For a given v, this solution is completely determined by the boundary conditions at the tip of the rupture: $u(0)=u'(0)=u''(0)=0$. When—and if—this solution reaches a point where $\dot{u}=vu'=1/(2\alpha)$, it must join smoothly to a solution of (15) with $\phi=0$, that is, to a linear superposition of exponentials for which the three q's are the roots of

$$\eta v q^3-b^2q^2-1=0 . \tag{16}$$

For small η, these roots are $q\approx\pm i/b$ and $q\approx b^2/(\eta v)$. The first pair of these roots produces a sinusoidal front whose width is of order $b=(v^2-1)^{1/2}$, which we can understand to be a "relativistic" contraction of the characteristic scale length in this problem, defined earlier to be unity. The third root $q\approx b^2/(\eta v)$ produces a rapidly growing exponential which, if present with appreciable amplitude, would dominant the high-velocity solution and cause it either to decelerate rapidly and to rejoin the sticking family, or to accelerate rapidly and become entirely unphysical. Thus the edge solution, shown by the dashed curve in Fig. 2, must be at or near the propagation speed v for which the amplitude of this third mode, determined by the matching conditions at $\dot{u}=1/(2\alpha)$, passes through zero. The value of v at which this happens obviously cannot be less than that for which $\dot{u}_{\max}=1/(2\alpha)$. It also cannot be much greater than this value because, as seen in Fig. 2, the more rapidly accelerating solutions of (15) at small $\dot{u}$ cross over to divergent high-velocity solutions. Therefore, the LT guess turns out to be accurate even if not correct in the most fundamental sense.

We need now to reexamine the LT analysis of how the selection mechanism at $\epsilon>0$ merges with marginal stability at $\epsilon=0$. Of course, if the edge solution is always marginally stable, consistency is automatic. But we can say more. For analytic simplicity, consider the limiting case of small ϵ and η. The low-speed $[\dot{u}_{\max}<1/(2\alpha)]$, viscosity-dominated resticking solutions of (15) have the form

$$u(x)=-\epsilon+A_1e^{q_1x}+2\bar{A}e^{\bar{q}x}\cos(\tilde{q}x)+2\tilde{A}e^{\bar{q}x}\sin(\tilde{q}x) , \tag{17}$$

where q_1 and $\bar{q}\pm i\tilde{q}$ are the roots of (12) for some value of $v=v_c(\epsilon)$ [which, for small ϵ, we suppose to be just slightly smaller than $v_c(0)$], and where A_1 and $\bar{A}\pm i\tilde{A}$ are the amplitudes associated with those modes. To lowest order in η, we have $\bar{q}\approx(2\alpha/\eta)^{1/2}$ and $v_c^2(0)\approx1+2(2\alpha\eta)^{1/2}$, in accord with (13); we also find $q_1\approx1/(2\alpha)$ and $\tilde{q}\approx(8\alpha/\eta^3)^{1/4}[v_c(0)-v_c(\epsilon)]^{1/2}$. We see immediately that we need $v_c(\epsilon)<v_c(0)$ in order that the double root of (12) at $\epsilon=0$ becomes a complex-conjugate pair of roots for $\epsilon>0$. In this way, we obtain an oscillation in $u(x)$, and, thus, a (nominal) resticking point. Because the term $\exp(\bar{q}x)$ in (17) grows rapidly, the resticking point and the point at which $\dot{u}=vu'$ is maximum both must lie very close to $\bar{x}_r=\pi/\tilde{q}$. According to the preceding discussion, we should be able to determine v by setting $\dot{u}_{\max}=vu'(\bar{x}_r)\approx1/(2\alpha)$. The result is

$$v_c(\epsilon)\approx v_c(0)-\pi^2\left[\frac{\alpha\eta}{2}\right]^{1/2}\Big/\ln^2\left[\frac{1}{\epsilon}\right] , \tag{18}$$

$$\bar{x}_r\approx\left[\frac{\eta}{2\alpha}\right]^{1/2}\ln\left[\frac{1}{\epsilon}\right] . \tag{19}$$

Thus, $v_c(\epsilon)$ approaches the marginal-stability value $v_c(0)$ logarithmically in ϵ as $\epsilon\to0$, and $\bar{x}_r$, the distance between the front of the pulse and the nominal resticking point, diverges in this limit in accord with our picture of a purely exponential front at threshold.

Of course, we know from an examination of Fig. 2 that the actual resticking point x_r lies well beyond the nominal resticking point $\bar{x}_r$ and that, except possibly for very small values of ϵ, it is in the latter region that most of the slipping takes place. Away from threshold, the dynamically selected rupture front is the one for which the fault is locally slipping almost freely, unhindered by friction because $\dot{u}\gg1/(2\alpha)$. Thus viscosity does not play an important role during this phase of the motion because the selection mechanism guarantees that the fast mode with $q\approx b^2/(\eta v)$ is very nearly absent. To a good approximation, therefore, we can compute $u(x)$ by solving (17) with η and ϕ both set to zero. The result is (with $\Delta\equiv1-\epsilon$)

$$u(x)\approx\Delta\left[1-\cos\frac{x}{b}\right] , \tag{20}$$

from which we see again that the width W of the front is

$$W\approx\pi b=\pi[v_c^2(\epsilon)-1]^{1/2} . \tag{21}$$

This approximation is tested in Fig. 5, where we have plotted $W(v)$ as obtained from dynamic simulations along with the prediction (21). The residual discrepancy between the actual and predicted pulse widths occurs be-

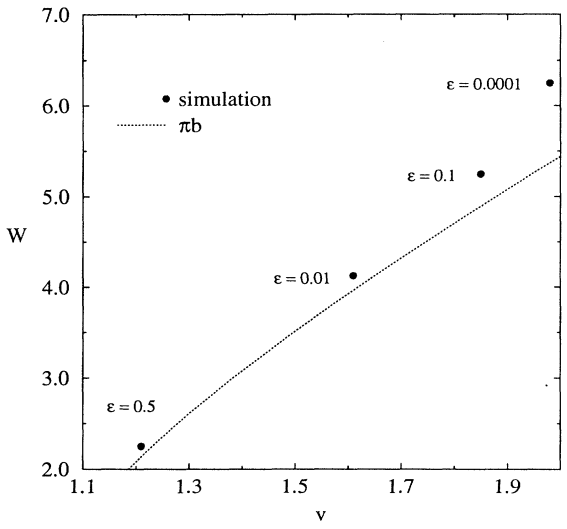

FIG. 5. Width W of the slip pulse (distance between the rupture tip and the resticking point) as a function of v, for $\alpha=3.0$ and $\eta=0.1$, at the values of ϵ indicated. Shown also is the dominant contribution to the pulse width from the regime where $\dot{u}>1/(2\alpha)$: $\pi b=\pi(v^2-1)^{1/2}$. The contribution from πb becomes less important as $\epsilon\to0$ and the rupture tip extends further out into the region ahead of the front.

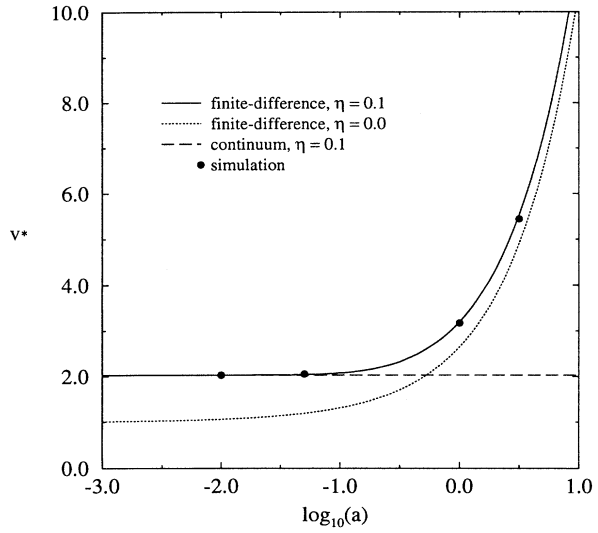

FIG. 6. Rupture velocity v^* predicted from linear marginal stability [Eq. (7)] at threshold ($\Delta=1$), as a function of grid spacing a for the finite-difference viscous model (14) (solid curve), the finite-difference BK model (4) (dotted curve), and the continuum viscous model (10) (dashed curve). Symbols represent velocities measured in simulations of the model for various a. All results are for $\alpha=3.0$ and $\eta=0.1$. The intermediate region where $\alpha\approx[\eta/(2\alpha)]^{1/2}$ is not described well by either limiting case, but the simulation results are accurately described for all a by the finite-difference viscous model with both length scales included.

cause (20) and (21) omit the viscosity-controlled regions of large acceleration at the beginning and end of the slipping zone. This effect is most pronounced near threshold ($\epsilon\approx 0$) where the width W of the slipping region diverges.

This picture of a rupture propagating in the form of a localized pulse of nearly free slip is similar to the notions of "Heaton pulses" [12] or "Schallamach waves" [16]. In such phenomena, parallel surfaces, such as a carpet on a floor or the two sides of an earthquake fault, move across one another not by uniform sliding, which requires a large amount of work, but by propagation of sharp pulses within which the surfaces effectively disengage. That is essentially the situation that emerges in the present model. A large amount of slip is achieved with little frictional drag—since the slip rate $\dot{u}$ is so large—and with little viscous dissipation—since the pulse resticks in a manner which minimizes the effect of this term. Although the uniform sliding mode seems intuitively simple and appealing, our analysis reveals that the dynamical mechanism for selecting the speed and the shape of these pulses, or even for predicting the conditions under which they may exist, is highly nontrivial.

IV. VISCOELASTICITY

The results obtained so far, like those in LT, have the apparently awkward feature that rupture speeds can exceed the sound velocity. This feature is a result of our having used a viscosity in (10) that is more appropriate for a liquid than a solid. In particular, (10) does not describe correctly the high-frequency response of an elastic material.

A more nearly correct constitutive relation for use in (10) would be one in which the instantaneous viscosity η is replaced by a time-delayed response:

$$\eta\frac{\partial^2\dot{u}}{\partial x^2}\rightarrow\int_{-\infty}^{t}\tilde{\eta}(t-t')\frac{\partial^2\dot{u}(t')}{\partial x^2}dt' \ . \tag{22}$$

To see the physical implication of (22), it is sufficient to suppose that $\tilde{\eta}$ is characterized by a single new exponential relaxation time τ, such that

$$\tilde{\eta}(t)=\frac{\eta}{\tau}\exp(-t/\tau) \ . \tag{23}$$

The symbol η now denotes the ordinary liquidlike viscous coefficient for processes that occur on time scales much longer than τ, in a manner consistent with its usage in Eq. (10).

The existence of a nonzero τ is essential in order to obtain a solidlike response at high frequencies. A good way to see this is to compute the sound speed in a uniform system governed by (10) but with the modified viscoelastic force given by (22) and (23) and without the friction ϕ. If $u\sim\exp(ikx+i\omega t)$, then the relation between the frequency ω and the wave number k can be written in the form

$$\omega^2=k^2\left[1+\frac{i\omega\eta}{1+i\omega\tau}\right] , \tag{24}$$

where we have assumed $k\gg 1$. For small enough k such that $\omega\tau\ll 1$, we find a damped wave with

$$\omega\approx k\left[\pm\left[1-\frac{\eta^2}{4}\right]^{1/2}+\frac{i\eta}{2}\right], \quad \omega\tau\approx k\tau\ll 1 \ . \tag{25}$$

The associated wave speed is of order unity for small η. At high frequencies, on the other hand, the damping disappears and we have

$$\omega\approx\pm k\left[1+\frac{\eta}{\tau}\right]^{1/2}, \quad \omega\tau\approx k\tau\left[1+\frac{\eta}{\tau}\right]^{1/2}\gg 1 \ . \tag{26}$$

Note that the high-frequency "unrelaxed" wave speed diverges as τ becomes small. In Sec. III, we have set $\tau=0$, so that this upper speed does not appear in that model. It is this speed, however, that limits the rate at which energy and momentum can flow through the solidlike material and therefore, it is this speed that would be an upper bound for rupture propagation.

The obvious question is whether the front of the rupture in our model is probing the viscoelastic response function $\tilde{\eta}$ at effectively high frequencies or low frequencies. Because we have set $\tau=0$ in Sec. III, we have implicitly assumed the latter, and we must now check this assumption for self-consistency. The largest characteristic frequencies of interest are of order q^*v. Using the results of Eq. (13) for small η, we find that self-consistency requires that

$$\omega\tau\approx q^*v\tau\approx\left[\frac{\alpha\tau^2}{\eta}\right]^{1/2}\ll 1 \ . \tag{27}$$

It follows that the model, as we have used it, makes good sense as long as the relaxation times or equivalently, in our units, the characteristic lengths τ and η are both small compared to α^{-1}, and as long as τ is not anomalously much larger than η. These seem to be reasonable assumptions. In this case, although $(q^*)^{-1} \sim [\eta/(2\alpha)]^{1/2}$ is small, the requirement $\omega\tau \sim (\alpha\eta)^{1/2} \ll 1$ becomes increasingly well satisfied as $\eta \to 0$.

V. COMPARISON OF VISCOUS AND FINITE-DIFFERENCE MODELS

The purpose of these calculations has not just been to solve for the rupture dynamics in the viscous model, but to begin to understand more generally the role of small length scales in these types of stick-slip models.

We have seen in Eqs. (9) and (13) that the selected quantities q^* and v^* scale differently with the two small scales in question, a and η. Therefore, the control of rupture dynamics by a small length scale depends on more than the magnitude of the cutoff. The specific details of this control depend on the manner in which the cutoff enters the dynamical equations of motion.

We have addressed here only questions pertaining to the dynamics of propagation along a uniformly stressed fault, which has been shown in previous studies of the uniform BK model [2,3] to be associated with large events in the earthquake cycle. If displacements (and hence stresses) on the fault are slightly irregular, and the fault is loaded over many cycles, then a broad distribution of event sizes is observed, such that the smallest events reflect the short-wavelength cutoff in the model. Simulations of the viscous model (14) carried out over many loading cycles [17] likewise reveal a broad distribution of earthquake magnitudes, with a cutoff in the distribution at small sizes determined by the magnitude of the viscous parameter η rather than the grid spacing a as was the case in the previous model.

The dynamics of rupture propagation have been shown to be governed by the continuum equation of motion (10) when the smoothing length of order $(q^*)^{-1} \sim [\eta/(2\alpha)]^{1/2}$ is sufficiently larger than the grid spacing a that we introduced in our finite-difference approximation (14). This is because the motion of the front is smooth on the scale of $(q^*)^{-1}$ and cannot exhibit dynamical structure on the scale of the grid spacing a. We know, however, that in the limit $\eta \to 0$, we return to the original model (4) without any viscosity and must once again become dependent on the underlying grid spacing.

In order to address this crossover from the continuum model dominated by the viscous length scale $(q^*)^{-1}$ to the finite-difference model dominated by the grid spacing a, we can solve the marginal stability equations (7) for motion at threshold, using the finite-difference version of the viscous model (14), where Ω is the solution of

$$\Omega^2 - 2\alpha\Omega + 1 - \frac{2}{a^2}[\cosh(qa) - 1](1 + \eta\Omega) = 0 . \quad (28)$$

We have solved Eqs. (7) and (28) and plotted in Fig. 6 the marginally stable velocity v^* as a function of the finite-difference grid spacing a for fixed η in the three cases of interest: the finite-difference viscous model ($\eta \neq 0$), the original finite-difference model ($\eta = 0$), and the continuum viscous model [$\eta \neq 0$, from the solution of Eqs. (7) and (11)]. The results of simulations are also shown for various a. In the intermediate region where $a \approx [\eta/(2\alpha)]^{1/2}$ neither of the limiting cases describes the rupture propagation very accurately.

VI. DISCUSSION AND CONCLUSIONS

We have investigated a simple extension of the uniform, one-dimensional Burridge-Knopoff model in which a small viscosity is introduced in order for the model to have a well-defined continuum limit, and have probed the manner in which the viscosity controls the dynamics of rupture propagation. We have examined in greater detail the process by which propagating modes are selected. In the off-threshold case, we have found a continuum of steady-state propagating modes, which is unusual for propagation into a metastable state. The off-threshold propagation is such that the system selects that mode which slips in a nearly free manner. The sharp pulses by which slip propagates in this model appear to be physically significant in a wide range of applications.

Our remaining point of greatest uncertainty is the mathematical mechanism for mode selection in the case of off-threshold slip. The situation is best summarized by a mode-counting analysis [18]. Near the tip of the crack at $x = 0$, where $u(x)$ is small, the solutions of the steady-state equation (15) have the form $u(x) = -\epsilon + \sum_{i=1}^{3} A_i \exp(q_i x)$, where the q_i are solutions of Eq. (12). For $v > 1$, all the q_i have positive real parts, and thus all three modes are allowed. The conditions $u(0) = u'(0) = u''(0) = 0$ fix the three amplitudes A_i, leaving only the parameter v unconstrained. Any solution of (15) from this one-parameter family of initial conditions will be continuous in all of its derivatives until the first place x_r where $u'(x_r) = 0$, at which point resticking occurs and $\phi(vu')$ takes on whatever value is needed to prevent back-slipping. For $x > x_r, u(\infty) \equiv u(x > x_r) = u(x_r)$ and, since we have no *a priori* information about the values of x_r or $u(\infty)$, we obtain no new constraint at the resticking point for determining v. If, however, we were to require that the front restick with a continuous second derivative $u''(x \to x_r -) = 0$, then the only acceptable solution would be the edge solution which resticks smoothly, and the velocity v would be constrained to be the critical velocity v_c. Nothing in our mathematics seems to require us to do this, but there are strong indications that both nature and our finite-difference integration scheme prefer this smooth solution.

Note that the situation is different at threshold. Since the three wave numbers q_i all have positive real parts and the rupture "tip" extends exponentially as $x \to -\infty$, all three modes $A_i \exp(q_i x)$ decay smoothly in this limit, and only one amplitude is therefore constrained by setting a reference point for the front. [For example, we can require $u'(0) = 1/(2\alpha v)$, thereby fixing an amplitude, say A_3, to be specific.] Then there remain three free parameters v, A_1, and A_2, which characterize a particular mode at threshold. Again, we can integrate (15) to the restick-

ing point and, if we allow any second derivative upon resticking, we continue to have a three-parameter family of solutions at threshold. If we require $u''(x_r)$ to be continuous, we are left with a two-parameter family of solutions. In either case, we are left with more than simply a one-parameter family of solutions characterized by the velocity v, which is typical for problems governed by linear marginal stability.

Other open questions remain. While we have shown (in Fig. 3) that initial conditions are attracted to the edge solution under the full time evolution of the dynamical model, we have not investigated in detail the stability of the more slowly moving subedge solutions, nor have we resolved the subtleties associated with representation of such singular solutions in our approximate numerical integrations. Therefore, we do not know if the state moving at $v=v_c$ is an isolated stable attractor at the edge of a continuous band of unstable steady-state solutions, or if that state resides at the edge of a band of stable steady-state solutions and is selected by some sort of marginal-stability mechanism. We have only noted that the selected mode is that for which the system slips in a nearly free manner, but we have not investigated to what extent such "disengagement" is an organizing factor in the dynamics of this system, or in other dynamical systems which exhibit localized failure. We have not investigated the effects of other physically relevant regularization schemes, such as a rate- and state-dependent friction force which introduces a characteristic slip distance [19], nor have we determined whether selection mechanisms of the type described here will persist in higher-dimensional generalizations of our fault model, where potentially singular elastic stress concentrations near the rupture tip could dominate the selection process.

ACKNOWLEDGMENTS

We would like to thank M. Barber, J. Carlson, P. Hohenberg, M. Marder, H. Nakanishi, J. Rice, B. Shaw, and C. Tang for useful conversations. This work was supported by DOE Grant No. DE-FG03-84ER45108 and NSF Grant No. PHY89-04035.

[1] R. Burridge and L. Knopoff, Bull Seis. Soc. Am. **57**, 341 (1967).
[2] J. M. Carlson and J. S. Langer, Phys. Rev. Lett. **62**, 2632 (1989); Phys. Rev. A **40**, 6470 (1989).
[3] J. M. Carlson, J. S. Langer, B. Shaw, and C. Tang, Phys. Rev. A **44**, 884 (1991).
[4] J. S. Langer and C. Tang, Phys. Rev. Lett. **67**, 1043 (1991).
[5] A. Kolmagorov, I. Petrovsky, and N. Piscounov, Bull. Univ. Moscow Ser. Int. Sec. A **1**, 1 (1937).
[6] D. G. Aronson and H. F. Weinberger, Adv. Math. **30**, 33 (1978).
[7] G. Dee and J. S. Langer, Phys. Rev. Lett. **50**, 383 (1983).
[8] E. Ben-Jacob, H. Brand, G. Dee, L. Kramer, and J. S. Langer, Physica D **14**, 348 (1985).
[9] W. van Saarloos, Phys. Rev. A **39**, 6367 (1989).
[10] W. van Saarloos and P. C. Hohenberg, Physica D **14**, 303 (1992).
[11] M. C. Cross and P. C. Hohenberg, Rev. Mod. Phys. (to be published).
[12] T. H. Heaton, Phys. Earth Planet Inter. **64**, 1 (1990).
[13] M. Barber, J. Donley, and J. S. Langer, Phys. Rev. A **40**, 366 (1989); J. S. Langer, *ibid.* **46**, 3123 (1992).
[14] The fact that the control parameter ϵ enters the model additively, rather than multiplicatively as in systems such as the complex Ginzburg-Landau equation (see Ref. [10]), means that for the case $\epsilon<0$, the fault is trivially unstable in that the uniform configuration $u=0$ will slip even in the absence of a propagating front.
[15] The case $\epsilon\neq 0$ differs from front propagation in other systems, such as the complex Ginzburg-Landau equation (see Ref. [10]), in that the rupture terminates at a definite point and does not decay exponentially ahead of the front. Only in the case $\epsilon=0$ does the rupture tip extend out indefinitely as such.
[16] A. Schallamach, Rubber Chem. Tech. **44**, 1147 (1971).
[17] J. M. Carlson (private communication).
[18] M. Barber (private communication).
[19] M. F. Linker and J. H. Dieterich, J. Geophys. Res. **97**, 4923 (1992), and references therein.